

1 **c-di-GMP-linked phenotypes are modulated by the interaction between a diguanylate  
2 cyclase and a polar hub protein**

3

4 Gianlucca G. Nicastro<sup>1</sup>, Gilberto H. Kaihami<sup>1</sup>, André A. Pulschen<sup>1</sup>, Jacobo Hernandez-  
5 Montelongo<sup>#2</sup>, Ana Laura Boechat<sup>1</sup>, Thays de O. Pereira<sup>1</sup>, Eliezer Stefanello<sup>1</sup>, Pio Colepicolo<sup>1</sup>,  
6 Christophe Bordi<sup>3</sup> and Regina L. Baldini\*<sup>1</sup>.

7

8 Departamento de Bioquímica, Instituto de Química, Universidade de São Paulo, Brazil <sup>1</sup>;  
9 Instituto de Física "Gleb Wataghin", Universidade Estadual de Campinas, Brazil <sup>2</sup>; Laboratoire  
10 d'Ingénierie des Systèmes Macromoléculaires, UMR7255 CNRS – Aix Marseille Université,  
11 France <sup>3</sup>. <sup>#</sup> Current address Departamento de Ciencias Matemáticas y Físicas, Facultad de  
12 Ingeniería, Universidad Católica de Temuco, La Araucanía, Chile.

13

14 Running title: FimV localizes and modulates DgcP activity

15

16 \* Address correspondence to Regina L. Baldini, [baldini@iq.usp.br](mailto:baldini@iq.usp.br).

17 Av. Professor Lineu Prestes, 748 sala 1211, São Paulo-SP, Brazil, 05508-000

18 Telephone : +55 11 30918992

19

20

21

22 **Summary**

23 c-di-GMP is a major player in the decision between biofilm and motile lifestyles.  
24 Several bacteria present a large number of c-di-GMP metabolizing proteins, thus a fine-tuning  
25 of this nucleotide levels may occur. It is hypothesized that some c-di-GMP metabolizing  
26 proteins would provide the global c-di-GMP levels inside the cell whereas others would  
27 maintain a localized pool, with the resulting c-di-GMP acting at the vicinity of its production.  
28 Although attractive, this hypothesis has yet to be proven in *Pseudomonas aeruginosa*. We  
29 found that the diguanylate cyclase DgcP interacts with the cytosolic region of FimV, a  
30 peptidoglycan-binding protein involved in type IV pilus assembly. Moreover, DgcP is located  
31 at the cell poles in wild type cells, but scattered in the cytoplasm of cells lacking FimV.  
32 Overexpression of DgcP leads to the classical phenotypes of high c-di-GMP levels (increased  
33 biofilm and impaired motilities) in the wild-type strain, but not in a  $\Delta fimV$  background.  
34 Therefore, our findings strongly suggest that DgcP is regulated by FimV and may provide the  
35 local c-di-GMP pool that can be sensed by other proteins at the cell pole, bringing to light a  
36 specialized function for a specific diguanylate cyclase.

37 **Introduction**

38 Over the past decades, (3'-5')-cyclic diguanylic acid (c-di-GMP) has been  
39 characterized as an important second messenger in bacteria. The concentration of c-di-GMP  
40 within the cell is associated with cellular behavior: high c-di-GMP levels are linked to biofilm  
41 formation and low levels to the motile planktonic lifestyle (Simm *et al.*, 2004; Romling *et al.*,  
42 2013). This molecule is synthesized from GTP by a class of enzymes known as diguanylate  
43 cyclases (DGC) bearing a conserved GGDEF motif (Chan *et al.*, 2004). The c-di-GMP  
44 hydrolysis reaction is performed by phosphodiesterases (PDE) with EAL or HD-GYP domains,  
45 which cleave c-di-GMP to pGpG or GMP, respectively (Schmidt *et al.*, 2005; Ryan *et al.*,

46 2006). Multiple genes coding for the c-di-GMP-metabolizing proteins are found in a variety of  
47 bacterial genomes. A puzzling question in the study of c-di-GMP signaling is how the bacterial  
48 cell integrates the contributions of multiple c-di-GMP-metabolizing enzymes to mediate its  
49 cognate functional outcomes. Merritt and collaborators showed that the *P. aeruginosa*  
50 phenotypes controlled by two different DGC have discrete outputs despite the same level of  
51 total intracellular c-di-GMP (Merritt *et al.*, 2010). These data support the model in which  
52 localized c-di-GMP signaling contributes to the action of proteins involved in the synthesis,  
53 degradation, and/or binding to a downstream target (Romling *et al.*, 2013). Studies of c-di-  
54 GMP signaling regulation during the swarmer to stalked-cell transition in *Caulobacter*  
55 *concentus* also supports this hypothesis. In this dimorphic bacterium, PleD is a DGC that is  
56 inactive in swarmer cells and is activated during the swarmer-to-stalked cell differentiation  
57 (Aldridge *et al.*, 2003; Paul *et al.*, 2004). Activation of PleD is coupled to its subcellular  
58 localization at the stalk pole, suggesting that PleD activates nearby downstream effectors  
59 involved in pole remodeling (Paul *et al.*, 2007). Opposite to PleD, the EAL domain protein  
60 TipF localizes at the swarmer pole, where it contributes to the proper placement of the motor  
61 organelle in the polarized predivisional cell (Davis *et al.*, 2013).

62 Even though a large body of research on c-di-GMP regulation in *P. aeruginosa* is  
63 available, it is still unclear whether compartmentalization of c-di-GMP signaling components is  
64 required to mediate an appropriate c-di-GMP signal transduction. The genome of *P.*  
65 *aeruginosa* strain PA14 presents forty genes coding for proteins associated with c-di-GMP  
66 metabolism (Kulasakara *et al.*, 2006; Lee *et al.*, 2006). Some of these proteins were already  
67 characterized and a few of them present a specific localization within the cell. For instance,  
68 the DGC WspR is associated to contact-dependent response to solid surfaces. Activation of  
69 the Wsp system by contact leads to the formation of subcellular clusters of WspR followed by

70 synthesis of c-di-GMP, increasing exopolysaccharide production and biofilm formation  
71 (Huangyutitham *et al.*, 2013). The DGC SadC is a central player in Gac/Rsm-mediated biofilm  
72 formation (Moscoso *et al.*, 2014) and influences biofilm formation and swarming motility via  
73 modulation of exopolysaccharide production and flagellar function (Merritt *et al.*, 2007).  
74 Recently, it was demonstrated that SadC activity is promoted by membrane association, with  
75 the formation of active DGC oligomers (Zhu *et al.*, 2016). The PDE DipA/Pch is essential for  
76 biofilm dispersion (Roy *et al.*, 2012) and promotes c-di-GMP heterogeneity in *P. aeruginosa*  
77 population (Kulasekara *et al.*, 2013). This PDE is partitioned after cell division and is localized  
78 to the flagellated cell pole by the chemotaxis machinery. This asymmetric distribution during  
79 cell division results in a bimodal distribution of c-di-GMP (Kulasekara *et al.*, 2013).

80 Previously, we demonstrated that PA14\_72420 is an enzymatically active DGC that  
81 increased imipenem fitness (Nicastro *et al.*, 2014). Although this protein has been the subject  
82 of recent publications that named it as DgcP (Aragon *et al.*, 2015), its molecular function has  
83 not yet been addressed. Thus, we decided to pursue its role by seeking for DgcP interaction  
84 partners that could participate in the same signaling pathway. DgcP was found to interact with  
85 the inner membrane protein FimV, which has a regulatory role in type IV pilus (T4P) function.  
86 Moreover, we determined that DgcP localizes to cell poles in a FimV-dependent manner and  
87 is more active when the FimV protein is present. We suggest that the DgcP regulation by  
88 FimV may provide a local c-di-GMP pool at the cell pole, making this second messenger  
89 available for the c-di-GMP binding proteins that may regulate the machineries associated with  
90 the cell motility, such as the flagellum and pili.

91 **Results**

92 **DgcP interacts with FimV.** One of the interesting paradoxes of signal transduction by  
93 c-di-GMP is the redundancy of DGCs and PDEs in bacterial cells. It has been shown that

94 distinct phenotypes are controlled by specific DGCs or PDEs (Merritt *et al.*, 2010; Romling *et*  
95 *al.*, 2013). The specificity of DGCs and PDEs has been proposed to be related to protein  
96 localization, allowing the regulation of subcellular pools of c-di-GMP close to a target receptor  
97 (Merritt *et al.*, 2010; McDougald *et al.*, 2012). Therefore, we sought, using bacterial two-hybrid  
98 system, for interaction partners of DgcP that could give a hint of DgcP localization and  
99 function. The bait plasmid pKT25\_dgcP was constructed with the complete *dgcP* coding  
100 region (**Fig. 1 A**) and co-transformed in BTH101 *E. coli* cells with a *P. aeruginosa* fragment  
101 prey library cloned in the pUT18C plasmid (Houot *et al.*, 2012). About 100,000 co-  
102 transformants were obtained and 40 positive red colonies identified. All positives clones were  
103 retested by individually transforming different pUT18 derivative preys and the pKT25\_dgcP or  
104 pKT25 empty vector plasmids into BTH101 cells. From the 40 clones initially obtained, 26  
105 were confirmed and the inserts were further identified by DNA sequencing. Only two clones  
106 presented *in frame* inserts, one of them corresponding to a short peptide fragment (36 amino  
107 acids) of the cytoplasmic, C-terminal portion of FimV (**Fig. 1 B**, red box). FimV is a large  
108 protein (924 amino acids, 97 kDa) containing a periplasmic domain with a peptidoglycan-  
109 binding LysM motif connected via a single transmembrane segment to a highly acidic  
110 cytoplasmic domain with three predicted protein-protein interaction tetratricopeptide repeat  
111 (TPR). FimV is part of the T4P secretion machinery in *Pseudomonas* (Wehbi *et al.*, 2011) and  
112 is required for localization of some T4P assembly components to the cell pole (Carter *et al.*,  
113 2017). As T4P are important for initial cell attachment and the  $\Delta dgcP$  mutant is impaired in  
114 this trait (Aragon *et al.*, 2015), we decided to further investigate the interaction of FimV with  
115 DgcP. Two constructs, one containing the FimV cytoplasmic region and the other, a smaller  
116 cytoplasmic fragment were cloned into pUT18 plasmid (**Fig. 1 B**). After co-transformation of  
117 each of these plasmids with pKT25\_dgcP in BTH101 cells, we confirmed that DgcP interacts

118 with the cytoplasmic region of FimV (**Fig. 1 C and D**). Stronger interactions were observed  
119 with the constructs containing the prey fragment or the full cytoplasmic region.

120 **FimV localizes DgcP at the cell poles.** Type IV pili are surface appendages that  
121 localize at the cell poles in *P. aeruginosa*. There are several polar localized proteins involved  
122 in the assembly and regulation of the T4P system and FimV is one of them (Wehbi *et al.*,  
123 2011; Inclan *et al.*, 2016; Buensuceso *et al.*, 2016). Due to its interaction with FimV, we asked  
124 whether DgcP would also localize at the cell poles. Indeed, when cells overexpresses the  
125 fusion protein DgcP-msfGFP, polar fluorescent foci were observed in virtually 100% of both  
126 PA14 (not shown) and  $\Delta$ dgcP strains (**Fig. 2 A**). This localization is lost when DgcP-msfGFP  
127 is expressed in a  $\Delta$ fimV mutant, where the fluorescence is scattered throughout the cells (**Fig.**  
128 **2 B and C**). To narrow the DgcP region important to the interaction, we use two different  
129 DgcP-msfGFP fusions, one containing the first 199 amino acids (N-ter-DgcP-msfGFP) and  
130 the other the last 461 amino acids (C-ter-DgcP-msfGFP) (**Fig. 2 A**). The C-terminal fusion  
131 fluorescence was scattered in the cells (not show) and cells overexpressing the N-ter-DgcP-  
132 msfGFP presented a growth defect, precluding its analysis. Therefore, we cannot determine  
133 precisely which region of DgcP is important to polar localization.

134 As the DgcP C-terminal construct is not localized and there are no predicted domains  
135 in the N-terminal region, we aligned 85 sequences of putative DgcP orthologues from 75  
136 species, including 53 Pseudomonadaceae and 32 other proteobacteria, such as Vibrionales  
137 and Alteromonadales (**Table S2**). We found that the N-terminal region is composed by two  
138 separate conserved segments (**Fig. S1**) and both or one of them may be responsible for  
139 interaction with FimV, which homologues are present in all those bacterial genomes.

140 **DgcP plays a role in biofilm formation.** The role of DgcP in biofilm formation has  
141 been investigated by different groups under different conditions. Kulasekara and collaborators

142 showed that mutation in DgcP abolished biofilm formation in LB medium (Kulasakara *et al.*,  
143 2006) and Ha and collaborators showed that a *dgcP* mutation did not affect biofilm formation  
144 in M63 minimum medium (Dae-Gon Ha *et al.*, 2014). Aragon and collaborators demonstrated  
145 that deletion of *dgcP* orthologues in *Pseudomonas savastanoi* pv. *savastanoi* and *P.*  
146 *aeruginosa* PAK indeed decreased biofilm formation in LB (Aragon *et al.*, 2015). Here, we  
147 confirmed that the PA14  $\Delta dgcP$  mutant is impaired in biofilm formation in the rich medium LB,  
148 but minor differences were observed in minimal M63 medium (**Fig. 3 A**). These results are in  
149 agreement with the differences observed by the two previous studies (Kulasakara *et al.*, 2006;  
150 Dae-Gon Ha *et al.*, 2014). The expression *in trans* of *dgcP* restores the phenotype of biofilm  
151 defect on  $\Delta dgcP$  (**Fig. 3 B and C**). In LB,  $\Delta dgcP$  was not able to form a biofilm and just a few  
152 adherent cells were observed by confocal laser scanning microscopy (CLSM) after 16h post-  
153 inoculation, while the wild type PA14 biofilm was more developed at this time point (**Fig. 3 C**).  
154 At 72 hours,  $\Delta dgcP$  biofilm was thin and undifferentiated (**Fig. 3 D**). As FimV is also involved  
155 in biofilm formation (**Fig. 5**), this is another indication that they have complementary roles in  
156 the cells, probably related to the T4P function.

157 **DgcP has a role in twitching motility.** *P. aeruginosa* utilizes T4P to move across solid  
158 surfaces in a process known as twitching motility. As T4P are regulated by FimV, we decided  
159 to investigate if DgcP is important for twitching. A small portion of the outer edge of the  
160 bacterial streak was taken and stabbed into the bottom of the agar plate or placed on a thin  
161 layer of solidified media and covered with a glass coverslip. Cells were incubated and active  
162 colony expansion occurred at the interstitial interface. Twitching motility was analyzed by  
163 staining the plates with crystal violet after 16h (**Fig. 4 A and B**) or by phase contrast  
164 microscopy after 4 hours of colony expansion (**Fig. 4 C**). As expected, the  $\Delta dgcP$  mutant  
165 presented decreased twitching motility with a less defined structure whereas PA14 presented

166 a well-defined lattice-like network. The *fimV* mutant was not able to perform the twitching  
167 motility (**Fig. 4**), as expected (Semmler *et al.*, 2000). Initiation of biofilm formation was also  
168 analyzed after five hours of adhesion of cells on a silicon slide at the air-liquid interface. The  
169 cultures were adjusted to an  $OD_{600} = 0.05$  in M63 minimum medium supplemented with  
170 glucose and casamino acids. The silicon slide was placed upright in a culture tube and cells at  
171 the air-liquid interface were analyzed by field emission scanning electron microscope  
172 (FESEM), after different time points (**Fig. 4 D**). PA14 early biofilm presented an irregular  
173 architecture due to the motility of the initial adhering cells, but only round microcolonies that  
174 did not expand on the surface were observed for the  $\Delta dgcP$  mutant (**Fig. 4 D**). These results  
175 show that DgcP is important to early stages of biofilm formation and twitching motility.

176 **DgcP activity is FimV dependent.** Here we observed that the FimV protein localizes  
177 the diguanylate cyclase DgcP at the cell pole (**Fig. 2**). Thus, we asked whether DgcP activity  
178 could be regulated by FimV. To answer this question, we overexpressed the DgcP-msfGFP in  
179 the  $\Delta fimV$  mutant and analyzed the phenotypes related to c-diGMP. Overexpression of the  
180 DGCs DgcP and WspR fused to msfGFP in PA14 increases biofilm formation and decreases  
181 swimming motility, indicating that these fusions are functional. Both DGCs also complement  
182 the  $\Delta dgcP$  mutation, but DgcP-msfGFP is not able to increase biofilm formation or decrease  
183 swimming motility in the  $\Delta fimV$  background, suggesting that it needs FimV for full activity. This  
184 is not observed for WspR-msfGFP, which has the same effect with or without FimV in the  
185 cells. Overexpression of the C-terminal portion of DgcP (pDgcP-Cterm) that does not localize  
186 to the cell poles has no effect on biofilm formation and swimming motility (**Fig. 5 A and B**) in  
187 all strains tested, even though there is an increase in overall c-di-GMP levels (**Fig. 5 C**),  
188 suggesting that localization of the diguanylate cyclase activity is important for those  
189 phenotypes. Moreover, overexpression of a mutated DgcP in the diguanylate cyclase motif

190 (GGEEF to GGAAF) decreases biofilm formation in the wild type PA14, but has no effect on  
191 both  $\Delta dgcP$  and  $\Delta fimV$  backgrounds (**Fig. 5 A and B**). DGCs are dimeric proteins therefore  
192 the GGAAF mutation may act as a negative dominant on the wild type DgcP.

193 CdrA is a extracellular protein considered as a scaffold for the biofilm extracellular  
194 matrix and transcription of *cdrA* is c-di-GMP-dependent, via FleQ (Borlee *et al.*, 2010) and it is  
195 widely used as a reporter of c-di-GMP levels (Rybtko *et al.*, 2012). Overexpression of DgcP-  
196 msfGFP leads to ~10-fold increased *cdrA* mRNA levels in PA14 and  $\Delta dgcP$ , but only fourfold  
197 in the  $\Delta fimV$  strain (**Fig. 5 D**). Quantitation of c-di-GMP agrees with the *cdrA* expression levels  
198 (**Fig. 5 C**). Exopolysaccharide (EPS) is also an indication of c-di-GMP levels in several  
199 bacteria (Chen *et al.*, 2014; Reichhardt *et al.*, 2015). DgcP and FimV were overexpressed  
200 alone or in combination in *Escherichia coli* cells and the production of EPS was assessed in  
201 Congo red plates. FimV overexpression does not result in EPS production, but colonies  
202 overexpressing DgcP have a pale tint. When both proteins are overexpressed together, EPS  
203 production increases, resulting in pink colonies (**Fig. 5 E**). Altogether, our results corroborate  
204 the hypothesis that the polar localization of DgcP by FimV also regulates its activity and that  
205 DgcP may contribute to a local c-di-GMP pool.

206 **Discussion**

207 Recently, Aragon and collaborators showed that DgcP is a well conserved DGC protein  
208 in Pseudomonads related to plant and human infections (Aragon *et al.*, 2015). Previously, we  
209 showed that overexpression of this protein alters biofilm formation, swimming and swarming  
210 motilities as well as imipenem fitness, due to reduced levels of OprD (Nicastro *et al.*, 2014).  
211 However, we could not conclude that those phenotypes were specifically related to the  
212 physiological role of DgcP, because it was assumed that the overexpression of a DGC  
213 increases the global c-di-GMP levels. Herewith, we used protein-protein interactions,

214 characterization of a deletion mutant and protein localization to look for the specific function of  
215 DgcP.

216 *P. aeruginosa* possesses polar T4P which are used for twitching motility and adhesion  
217 (Burrows, 2012), essential traits for mature biofilm architecture. Assembly of T4P at normal  
218 conditions requires FimV (Wehbi *et al.*, 2011), which shares similar domain organization with  
219 *Vibrio cholerae* HubP. These proteins, despite low overall sequence similarity, present a  
220 conserved N-terminal periplasmic domain required for polar targeting, and a highly variable C-  
221 terminal acidic cytoplasmic region, implicated in protein-protein interactions. HubP is required  
222 for polar localization of the chromosomal segregation and chemotactic machineries (Yamaichi  
223 *et al.*, 2012; Rossmann *et al.*, 2015). We found that DgcP is present only at the cell poles and  
224 that this pattern is dependent on FimV. Thus, we hypothesized that DgcP localization is  
225 important for the formation of a localized c-di-GMP pool at the cell poles that would assist the  
226 assembly and/or function of the T4P apparatus or other pole-localized organelles (**Fig. 6**). We  
227 suggest that DgcP could be one of the sources of c-di-GMP required for pilus biogenesis in *P.*  
228 *aeruginosa* and probably in other gamma-proteobacteria that carry DgcP and FimV homologs.

229 Assembly of *P. aeruginosa* T4P at normal conditions requires FimX, a polarly localized  
230 c-di-GMP binding protein (Jain *et al.*, 2012) that has degenerate DGC and PDE domains and  
231 seems to be enzymatically inactive (Navarro *et al.*, 2009). It is possible that binding of c-di-  
232 GMP to the EAL domain of FimX implicates it as an effector protein rather than a PDE, and a  
233 FimX mutant that does not bind c-di-GMP fails to activate PilB and twitching motility  
234 (Kazmierczak *et al.*, 2006). The FimX homolog in *Xanthomonas citri* interacts with a PilZ  
235 protein required for surface localization and assembly of pilin, but does not bind c-di-GMP  
236 (Guzzo *et al.*, 2013). *X. citri* PilZ subsequently interacts with PilB, an ATPase required for T4P  
237 polymerization, in a cascade of protein-protein interactions (Guzzo *et al.*, 2009; Dunger *et al.*,

238 2014). Remarkably, suppressor mutations in a *P. aeruginosa* *fimX* mutant that restored T4P  
239 biogenesis and partially restored twitching motility also increased c-di-GMP levels. However,  
240 the suppressor mutant cells presented peritrichous pili (Jain *et al.*, 2012), suggesting that, in  
241 addition to FimX, a more specific source of c-di-GMP would be needed for the correct  
242 assembly of the machinery at the cell poles. Similarly, a *P. aeruginosa* PilZ domain protein is  
243 also involved in the T4P-based twitching motility and does not bind to c-di-GMP, suggesting a  
244 conserved mechanism (Burrows, 2012). Cumulatively, these findings imply that the molecular  
245 mechanisms of pilus protrusion and retraction are regulated by local fluctuations of c-di-GMP  
246 levels. Other components of polar localized structures, such as flagella and the chemotactic  
247 machinery also bind directly or indirectly to c-di-GMP (Düvel *et al.*, 2012; Baker *et al.*, 2016),  
248 and DgcP may have a function in those mechanisms as well, but further work would be  
249 needed to uncover such roles.

250 *P. aeruginosa* T4P was demonstrated to be important not only to attach and move, but  
251 also to sense mechanical features of the environment. T4P sensing on solid surface  
252 increases its extension and retraction frequencies and cAMP production, leading to the  
253 upregulation of the cAMP/Vfr-dependent pathway (Persat *et al.*, 2015). Recently, FimV was  
254 associated with this process by interaction with FimL, a scaffold protein that connects T4P  
255 with the Chp chemosensory system via interaction with PilG and FimV (Inclan *et al.*, 2016;  
256 Buensuceso *et al.*, 2016). FimV is also involved in the transcriptional upregulation of *pilY1*,  
257 and PilY1 increases the SadC diguanylate cyclase activity upon surface contact (Luo *et al.*,  
258 2015). However, SadC presents localized foci at the poles, in the middle of cells and between  
259 these two locations (Zhu *et al.*, 2016), suggesting that it may have a broader role. Thus, we  
260 suggest that an outside signal could be sensed by T4P and transduced by FimV as described  
261 for SadC, resulting in the direct and localized activation of c-di-GMP production by DgcP. The

262 finding that FimV-DgcP interact at the poles is an important step towards the understanding of  
263 how c-di-GMP localized pools are formed, controlling the spatial activity of target proteins.

264

265 **Experimental procedures**

266       **Bacterial strains, plasmids and growth conditions.** The bacterial strains and  
267       plasmids used in the study are described in the Supplementary **Table S2**. For routine cell  
268       cultures, bacteria were grown aerobically in Luria–Bertani (LB) broth or LB agar at 37 or 30°C.  
269       Ampicillin (100 µg/ ml), kanamycin (50 µg/ml) or gentamicin (10 µg/ml) were added to  
270       maintain the plasmids in *E. coli*. Carbenicillin (300 µg/ ml), kanamycin (250 µg/ml) or  
271       gentamicin (50 µg/ml) were added to maintain the plasmids in *P. aeruginosa*. For the pJN105  
272       related constructs (**Table S1**), arabinose was added to cultures at 0.2 % final concentration.  
273       Both M8 (Kohler *et al.*, 2000) and M63 (Pardee *et al.*, 1959) minimal salt media were  
274       supplemented with 1mM MgSO<sub>4</sub>, 0.2 % glucose and 0.5 % casamino acids (CAA). To  
275       visualize bacterial two-hybrid interactions on solid medium, MacConkey indicator medium  
276       (Difco) supplemented with 1 % maltose and 100 mM IPTG (Isopropyl β-D-1-  
277       thiogalactopyranoside), herein designated MacConkey medium, was used.

278       **General molecular techniques.** DNA fragments were obtained by PCR using Q5 DNA  
279       polymerase (NEB). Oligonucleotide primers were purchased from Life Technologies and the  
280       sequences are listed in **Table S1**. PCR products of the expected sizes were purified from gels  
281       using GeneJET TM Gel Extraction Kit (Thermo Scientific), cloned using the SLIC method  
282       (Jeong *et al.*, 2012) and transformed into *E. coli* DH5α (**Table S1**). Plasmid purification was  
283       performed with GeneJET Plasmid Miniprep kit (Thermo Scientific). Sequencing was carried  
284       out using the Big Dye terminator cycle sequencing kit (Applied Biosystems) using the facility  
285       of the Departamento de Bioquímica, IQ-USP (SP, Brazil).

286       To construct unmarked in-frame deletions, the upstream and downstream regions of  
287       the target gene were amplified and cloned into the pEX18Ap (*fimV*) or pKNG (*dgcP*). The  
288       resulting constructs were used to delete target genes on wild type PA14 genome by

289 homologous recombination. To construct the pDgcP plasmid the *dgcP* coding region was  
290 cloned in frame with a synthetic *msfGFP* gene into the pJN105 plasmid. The *msfGFP* codes  
291 for a N-terminal 40 amino acids spacer and a C-terminal monomeric super fold GFP. All  
292 vectors and constructs are described in more detail in **Table S1**.

293 **Biofilm assays.** Three different biofilm assays were performed. The microtiter dish  
294 biofilm formation assay was performed as described (O'Toole, 2011). The biofilms observed  
295 by confocal laser scanning microscopy (CLSM) were grown in 8-well chamber slides and  
296 stained with DAPI as described (Jurcisek *et al.*, 2011) and imaged using a Zeiss - LSM 510-  
297 Meta. For the early stages of biofilm formation on silicon wafers, cultures were adjusted to an  
298 OD<sub>600</sub> = 0.05 in M63 medium and transferred to a 24-well plate where silicon slides (2x1 cm<sup>2</sup>)  
299 were placed upright in each well. Before using the silicon substrates, they were previously  
300 cleaned by ultra-sonication for a period of 15 min each in acetone, isopropanol and distilled  
301 water, respectively. Slides were dried under N<sub>2</sub> flow and subsequently treated with O<sub>2</sub> plasma  
302 at 100 mTorr for 15 min (720 V DC, 25 mA DC, 18 W; Harrick Plasma Cleaner, PDC-32G).  
303 After 60, 180 or 300 minutes the slides were rinsed three times with water, fixed with 4%  
304 paraformaldehyde for 1h and analysed by field-emission scanning electron microscopy  
305 (FESEM; model F50, FEI Inspect) operated at 2 keV. Prior to examination, samples were  
306 coated with sputtered gold to prevent electrical charging.

307 **High-throughput two-hybrid assays.** PAO1 two-hybrid library (Houot *et al.*, 2012)  
308 was tested against the pKT25\_DgcP bait. Basically, 25–50 ng of pUT18 library was  
309 transformed into BTH101 cells carrying the pKT25\_DgcP vector and plated on MacConkey  
310 medium for 48–96 h at 30 °C. Red colonies were picked up and restreaked on MacConkey  
311 plates. The positive colonies were cultivated in liquid medium, and plasmids were isolated and  
312 further analyzed. The candidate preys were retested individually for interaction with the bait by

313 retransforming pUT18 derivative prey and pKT25 bait plasmids into BTH101 cells and also  
314 the pUT18 derivative preys and the pKT25 empty vector. The interaction was evaluated by  
315 the color of spotted co-transformants on MacConkey plates and  $\beta$ -galactosidase assays.  
316 Cells were grown on MacConkey plates for 96 hours and they were scrapped and suspended  
317 in 1mL of PBS. 100  $\mu$ L were used in the classical  $\beta$ -galactosidase assay (Miller, 1972).

318 **Twitching assay.** Macroscopic twitching assay was performed as described (Dae-Gon  
319 Ha *et al.*, 2014) with minor modifications. Briefly, a colony was picked with a toothpick and  
320 stabbed at the bottom of a plate containing M8 medium supplemented with 1 mM MgSO<sub>4</sub>, 0.2  
321 % glucose, 0.5 % casamino acids and 2.0 % agar. The plates were incubated upright at 37°C  
322 overnight, followed by 48 h of incubation at room temperature (~25°C). Next, the agar was  
323 removed, and the bacteria were stained with 0.1% crystal violet. Microscopic twitching assay  
324 was performed as described (Turnbull and Whitchurch, 2014).

325 **Swimming assay.** Swimming assays were performed by inoculating 5  $\mu$ l of a  
326 stationary phase-grown liquid cultures in M8 with 0.3% agar that were incubated for 16 h at  
327 30°C in a plastic bag to maintain the humidity constant (Dae Gon Ha *et al.*, 2014).

328 **Congo red assay.** 5  $\mu$ l of stationary phase-grown cultures were inoculated at 1%  
329 agar plates of tryptone broth (10 g/L) containing Congo red (40  $\mu$ g/mL) and Coomassie  
330 brilliant blue (20  $\mu$ g/mL). The plates were incubated for 16 h at 30°C and then for 96 hours at  
331 room temperature.

332 **qRT-PCR.** For qRT-PCRs, total RNA was extracted with Trizol (Invitrogen), treated  
333 with DNase I (Thermo Scientific, Waltham, MA, USA) and used for cDNA synthesis with  
334 Improm II (Promega) or Superscript III (Invitrogen) and hexamer random primers (Thermo  
335 Scientific). cDNA was then amplified with specific primers using Maxima SYBRGreen/ROX

336 qPCR Master Mix (Thermo Scientific) and the 7300 Real Time PCR System (Applied  
337 Biosystems). *nadB* was used as internal control for normalization of total RNA levels  
338 (Lequette *et al.*, 2006). The relative efficiency of each primer pair was tested and compared  
339 with that of *nadB* and the threshold cycle data analysis ( $2^{-\Delta\Delta Ct}$ ) was used (Livak and  
340 Schmittgen, 2001). All reactions were performed in triplicates, the assays were repeated at  
341 least twice using independent cultures and the results of one representative experiment are  
342 shown, with average values of technical triplicates and error bars representing standard  
343 deviation of  $\Delta\Delta Ct$ .

344 **Fluorescence and light microscopy.** To verify the localization of DgcP\_msfGFP  
345 fusions, fluorescence microscopy was performed using a Nikon Eclipse TiE microscope  
346 equipped with a 25-mm SmartShutter and an Andor EMCCD i-Xon camera. For fluorescence  
347 microscopy and bright field microscopy, a Plan APO VC Nikon 100X objective (NA = 1.4) and  
348 a Plan Fluor Nikon 40X objective (NA = 1.3) were used. For membrane staining, cells were  
349 treated with 50  $\mu$ g/mL FM4-64 (Invitrogen). For phase contrast microscopy, a Plan APO  $\lambda$   
350 OFN25 Nikon 100X objective (NA = 1.45) was used. All microscopy assays were performed  
351 with immobilized cells on 25 % LB pads with 1.5% agarose. Image analyses were performed  
352 using the ImageJ (Schneider *et al.*, 2012) and MicrobeJ (Ducret *et al.*, 2016) softwares.

353 **c-di-GMP extraction and quantification.** c-di-GMP was extracted as described by  
354 (Irie and Parsek, 2014) with minor modifications. 50 mL of cultures were grown in M8 medium  
355 at 37°C and 200 rpm until reach  $OD_{600} = 1$ . Cells were collected by centrifugation  
356 resuspended in 500  $\mu$ L of M8 medium with 0.6 M perchloric acid. The tubes were incubated  
357 on ice for 30 minutes and then centrifuged at 20000  $g$  for 10 minutes. The pellets were used  
358 for protein quantitation and the supernatants were neutralized with 1/5 volume 2.5 M  $KHCO_3$ .  
359 The nucleotide extracts were centrifuged again and the supernatants were stored at -80 °C.

360 High-performance liquid chromatography (LC) was performed using the 1200 Infinity LC  
361 System (Agilent) that consists of a degasser, a quaternary pump, a thermostated autosampler  
362 (4°C) and a temperature (30°C)-controlled column compartment. This system was coupled to  
363 an 3200 Qtrap LC-MS/MS system equipped with an Electrospray Ionization source (ESI) (AB  
364 Sciex, USA). Analyst 1.4.2 software (AB Sciex, USA) was used to operate the equipment and  
365 calculate c-di-GMP concentrations.

366 Samples (injection of 10  $\mu$ L) were separated by a Phenomenex Synergi Hydro-RP  
367 column (150 $\times$ 2 mm, 4  $\mu$ m) using 0.1% formic acid in 15 mM ammonium acetate as mobile  
368 phase A and MeOH as mobile phase B at a flow rate of 0.3 mL min<sup>-1</sup>. The gradient program  
369 was 0 min 2 % B, 0.5 min 2 % B, 4.5 min 30 % B, 6.0 min 80 % B, 7.0 min 80% B, 7.01 min  
370 2% B and 14 min 2 % B. For quantification of c-di-GMP, the tandem mass spectrometry  
371 method multiple reaction monitoring (MRM) was used in negative mode. The following  
372 parameters were set: nebulizer, heated auxiliary and curtain gases (nitrogen) at 20, 30, 10,  
373 respectively; Turbo IonSpray voltage and temperature at -3,800 V and 250 °C, respectively;  
374 MRM transition (in m/z) 689.1 → 344.2 with a dwell time of 200 ms per transition; collision  
375 energy (CE) at -45 eV; and declustering potential at -53 V. An external standard curve was  
376 prepared for c-di-GMP in the MRM mode. The stock solution was diluted and the c-di-GMP  
377 peak area plotted against the nominal concentrations (16 to 2,000 ng mL<sup>-1</sup>).

378 **Multiple Sequence Alignment and secondary structure prediction.** Reciprocal  
379 best-hit search was performed as described before (Kohler et al., 2015). Briefly, the Kyoto  
380 Encyclopedia of Genes and Genomes (KEGG) database was initially used to search open-  
381 reading frames showing highest identity against DgcP (GenBank: ABJ14873.1). This search  
382 resulted in a list that was used to reciprocal search its highest identity orthologue in *P.*  
383 *aeruginosa* UCBPPA14 genome. In both searches the threshold for Smith-Waterman score

384 was 100, and the resulting best-best hit was filtered using a minimum 20% identity comparing  
385 the identified homologue against the DgcP. A list of all organisms that displays a DgcP  
386 homologue are listed in Supplemental **Table S1**. Redundant sequences were filtered using  
387 CD-Hit (Li and Godzik, 2006) with a maximum identity of 90% (**Table S1**). A multiple  
388 sequence alignment was performed using MUSCLE software (Edgar, 2004). The multiple  
389 sequence alignment was then visualized in the jalview (Waterhouse et al., 2009) and  
390 secondary structure analysis predicted with JPred (Drozdetskiy et al., 2015).

391 **Acknowledgments.**

392 We would like to thank A. Bisson-Filho for kindly providing the msGFP synthetic gene,  
393 D. Schechtman and M. Navarro for carefully reading the manuscript. We are also in debt with  
394 F. Gueiros-Filho, L. Zambotti-Villela and M.A. Cotta for assistance with fluorescence  
395 microscopy, mass spectrometry and electron microscopy, respectively. We acknowledge the  
396 National Nanotechnology Laboratory (LNNano, CNPEM) for granting access to the electron  
397 microscopy facilities.

398 Conceived and designed the experiments: GGN, CB and RLB. Performed the FESEM  
399 experiments: JHM. Performed two-hybrid screening: GGN and CB. Performed fluorescence  
400 and light microscopy: GGN and AAP. General molecular procedures: GGN, GHK, ALB and  
401 TOP. HPLC-MS/MS: ES. Contributed reagents/materials/analysis tools: RLB, CB, PC. Wrote  
402 the paper: GGN, RLB.

403 G.G.N. is supported by São Paulo Research Foundation (FAPESP) grant numbers:  
404 2013/02375-1 and 2014/02381-4.

405 R.L.B. is partially supported by National Council for Scientific and Technological  
406 Development (CNPq 307218/2014-7) a São Paulo Research Foundation (FAPESP  
407 2014/05082-8). grant allowed the work in RLB laboratory.

408 C.B. is supported by the ANR grants REGALAD ANR-14-CE09-0005-02.

409 The authors declare that there is no conflict of interest.

410

411

## References

412 Aldridge, P., Paul, R., Goymer, P., Rainey, P., and Jenal, U. (2003) Role of the GGDEF  
413 regulator PleD in polar development of *Caulobacter crescentus*. *Mol Microbiol* **47**: 1695–708.

414 Aragon, I.M., Pérez-Mendoza, D., Moscoso, J.A., Faure, E., Guery, B., Gallegos, M.-T., *et al.*  
415 (2015) Diguanylate cyclase DgcP is involved in plant and human *Pseudomonas* spp.  
416 infections. *Environ Microbiol* **17**: 4332–4351.

417 Baker, A.E., Diepold, A., Kuchma, S.L., Scott, J.E., Ha, D.G., Orazi, G., *et al.* (2016) A PilZ  
418 domain protein FlgZ mediates c-di-GMP-dependent swarming motility control in  
419 *Pseudomonas aeruginosa*. *J Bacteriol* JB.00196-16.

420 Borlee, B.R., Goldman, A.D., Murakami, K., Samudrala, R., Wozniak, D.J., and Parsek, M.R.  
421 (2010) *Pseudomonas aeruginosa* uses a cyclic-di-GMP-regulated adhesin to reinforce the  
422 biofilm extracellular matrix. *Mol Microbiol* **75**: 827–842.

423 Buensuceso, R.N.C., Nguyen, Y., Zhang, K., Daniel-Ivad, M., Sugiman-Marangos, S.N.,  
424 Fleetwood, A.D., *et al.* (2016) The conserved tetratricopeptide repeat-containing c-terminal  
425 domain of *Pseudomonas aeruginosa* FimV Is required for its cyclic AMP-Dependent and -  
426 independent functions. *J Bacteriol* **198**: 2263–74.

427 Burrows, L.L. (2012) *Pseudomonas aeruginosa* twitching motility: type IV pili in action. *Annu  
428 Rev Microbiol* **66**: 493–520.

429 Carter, T., Buensuceso, R.N.C., Tammam, S., Lamers, R.P., Harvey, H., Howell, P.L., and  
430 Burrows, L.L. (2017) The type IVa pilus machinery is recruited to sites of future cell division.  
431 *MBio* **8**: e02103-16.

432 Chan, C., Paul, R., Samoray, D., Amiot, N.C., Giese, B., Jenal, U., and Schirmer, T. (2004)  
433 Structural basis of activity and allosteric control of diguanylate cyclase. *Proc Natl Acad Sci U*

434 S A **101**: 17084–17089.

435 Chen, L.H., Köseoğlu, V.K., Güvener, Z.T., Myers-Morales, T., Reed, J.M., D’Orazio, S.E.F.,  
436 *et al.* (2014) Cyclic di-GMP-dependent signaling pathways in the pathogenic firmicute *Listeria*  
437 *monocytogenes*. *PLoS Pathog* **10**: e1004301.

438 Davis, N.J., Cohen, Y., Sanselicio, S., Fumeaux, C., Ozaki, S., Luciano, J., *et al.* (2013) De-  
439 and repolarization mechanism of flagellar morphogenesis during a bacterial cell cycle. *Genes*  
440 *Dev* **27**: 2049–62.

441 Ducret, A., Quardokus, E.M., and Brun, Y. V (2016) MicrobeJ, a tool for high throughput  
442 bacterial cell detection and quantitative analysis. *Nat Microbiol* **1**: 16077.

443 Dunger, G., Guzzo, C.R., Andrade, M.O., Jones, J.B., and Farah, C.S. (2014) *Xanthomonas*  
444 *citri* subsp. *citri* type IV Pilus is required for twitching motility, biofilm development, and  
445 adherence. *Mol Plant-Microbe Interact MPMI* **27**: 1132–1147.

446 Düvel, J., Bertinetti, D., Möller, S., Schwede, F., Morr, M., Wissing, J., *et al.* (2012) A chemical  
447 proteomics approach to identify c-di-GMP binding proteins in *Pseudomonas aeruginosa*. *J*  
448 *Microbiol Methods* **88**: 229–36.

449 Guzzo, C.R., Dunger, G., Salinas, R.K., and Farah, C.S. (2013) Structure of the PilZ-  
450 FimXEAL-c-di-GMP complex responsible for the regulation of bacterial type IV pilus  
451 biogenesis. *J Mol Biol* **425**: 2174–2197.

452 Guzzo, C.R., Salinas, R.K., Andrade, M.O., and Farah, C.S. (2009) PilZ protein structure and  
453 interactions with PilB and the FimX EAL domain: implications for control of type IV pilus  
454 biogenesis. *J Mol Biol* **393**: 848–866.

455 Ha, D.-G., Richman, M.E., and O’Toole, G.A. (2014) Deletion mutant library for investigation  
456 of functional outputs of cyclic diguanylate metabolism in *Pseudomonas aeruginosa* PA14.

457 *Appl Environ Microbiol* **80**: 3384–93.

458 Ha, D.G., Kuchma, S.L., and O'Toole, G.A. (2014) Plate-Based assay for swimming motility in  
459 *Pseudomonas aeruginosa*. *Methods Mol Biol* **1149**: 59–65.

460 Houot, L., Fanni, A., Bentzmann, S. de, and Bordi, C. (2012) A bacterial two-hybrid genome  
461 fragment library for deciphering regulatory networks of the opportunistic pathogen  
462 *Pseudomonas aeruginosa*. *Microbiology* **158**: 1964–1971.

463 Huangyutitham, V., Güvener, Z.T., and Harwood, C.S. (2013) Subcellular clustering of the  
464 phosphorylated WspR response regulator protein stimulates its diguanylate cyclase activity.  
465 *MBio* **4**: e00242-13.

466 Inclan, Y.F., Persat, A., Greninger, A., Dollen, J. Von, Johnson, J., Krogan, N., et al. (2016) A  
467 scaffold protein connects type IV pili with the Chp chemosensory system to mediate activation  
468 of virulence signaling in *Pseudomonas aeruginosa*. *Mol Microbiol* **101**: 590–605.

469 Irie, Y., and Parsek, M.R. (2014) LC/MS/MS-based quantitative assay for the secondary  
470 messenger molecule, c-di-GMP. *Methods Mol Biol* **1149**: 271–279.

471 Jain, R., Behrens, A.-J., Kaever, V., and Kazmierczak, B.I. (2012) Type IV pilus assembly in  
472 *Pseudomonas aeruginosa* over a broad range of cyclic di-GMP concentrations. *J Bacteriol*  
473 **194**: 4285–94.

474 Jeong, J.-Y., Yim, H.-S., Ryu, J.-Y., Lee, H.S., Lee, J.-H., Seen, D.-S., and Kang, S.G. (2012)  
475 One-step sequence- and ligation-independent cloning as a rapid and versatile cloning method  
476 for functional genomics studies. *Appl Environ Microbiol* **78**: 5440–3.

477 Jurcisek, J. a, Dickson, A.C., Bruggeman, M.E., and Bakaletz, L.O. (2011) *In vitro* biofilm  
478 formation in an 8-well chamber slide. *J Vis Exp* **47**: e2481.

479 Kazmierczak, B.I., Lebron, M.B., and Murray, T.S. (2006) Analysis of FimX, a

480 phosphodiesterase that governs twitching motility in *Pseudomonas aeruginosa*. *Mol Microbiol*  
481 **60**: 1026–1043.

482 Kohler, T., Curty, L.K., Barja, F., Delden, C. van, and Pechere, J.C. (2000) Swarming of  
483 *Pseudomonas aeruginosa* is dependent on cell-to-cell signaling and requires flagella and pili.  
484 *J Bacteriol* **182**: 5990–5996.

485 Kulasakara, H., Lee, V., Brencic, A., Liberati, N., Urbach, J., Miyata, S., et al. (2006) Analysis  
486 of *Pseudomonas aeruginosa* diguanylate cyclases and phosphodiesterases reveals a role for  
487 bis-(3'-5')-cyclic-GMP in virulence. *Proc Natl Acad Sci U S A* **103**: 2839–2844.

488 Kulasekara, B.R., Kamischke, C., Kulasekara, H.D., Christen, M., Wiggins, P.A., and Miller,  
489 S.I. (2013) c-di-GMP heterogeneity is generated by the chemotaxis machinery to regulate  
490 flagellar motility. *Elife* **2013**: e01402.

491 Lee, D.G., Urbach, J.M., Wu, G., Liberati, N.T., Feinbaum, R.L., Miyata, S., et al. (2006)  
492 Genomic analysis reveals that *Pseudomonas aeruginosa* virulence is combinatorial. *Genome*  
493 *Biol* **7**: R90.

494 Lequette, Y., Lee, J.H., Ledgham, F., Lazdunski, A., and Greenberg, E.P. (2006) A distinct  
495 QscR regulon in the *Pseudomonas aeruginosa* quorum-sensing circuit. *J Bacteriol* **188**: 3365–  
496 3370.

497 Livak, K.J., and Schmittgen, T.D. (2001) Analysis of relative gene expression data using real-  
498 time quantitative PCR and the 2(-Delta Delta C(T)) Method. *Methods* **25**: 402–8.

499 Luo, Y., Zhao, K., Baker, A.E., Kuchma, S.L., Coggan, K.A., Wolfgang, M.C., et al. (2015) A  
500 hierarchical cascade of second messengers regulates *Pseudomonas aeruginosa* Surface  
501 Behaviors. *MBio* **6**: e02456-14.

502 McDougald, D., Rice, S.A., Barraud, N., Steinberg, P.D., and Kjelleberg, S. (2012) Should we

503 stay or should we go: mechanisms and ecological consequences for biofilm dispersal. *Nat*  
504 *Rev Microbiol* **10**: 39–50.

505 Merritt, J.H., Brothers, K.M., Kuchma, S.L., and O'Toole, G.A. (2007) SadC reciprocally  
506 influences biofilm formation and swarming motility via modulation of exopolysaccharide  
507 production and flagellar function. *J Bacteriol* **189**: 8154–64.

508 Merritt, J.H., Ha, D.-G., Cowles, K.N., Lu, W., Morales, D.K., Rabinowitz, J., et al. (2010)  
509 Specific control of *Pseudomonas aeruginosa* surface-associated behaviors by two c-di-GMP  
510 diguanylate cyclases. *MBio* **1**: e00183-10-.

511 Miller, J.H. (1972) *Experiments in Molecular Genetics*. 2nd ed., Cold Spring Harbor  
512 Laboratory, Cold Spring Harbor, New York.

513 Moscoso, J.A., Jaeger, T., Valentini, M., Hui, K., Jenal, U., and Filloux, A. (2014) The  
514 diguanylate cyclase SadC is a central player in Gac/Rsm-mediated biofilm formation in  
515 *Pseudomonas aeruginosa*. *J Bacteriol* **196**: 4081–8.

516 Navarro, M.V.A.S., De, N., Bae, N., Wang, Q., and Sondermann, H. (2009) Structural analysis  
517 of the GGDEF-EAL domain-containing c-di-GMP receptor FimX. *Structure* **17**: 1104–16.

518 Nicastro, G.G., Kaihami, G.H., Pereira, T.O., Meireles, D.A., Groleau, M.C., Déziel, E., and  
519 Baldini, R.L. (2014) Cyclic-di-GMP levels affect *Pseudomonas aeruginosa* fitness in the  
520 presence of imipenem. *Environ Microbiol* **16**: 1321–1333.

521 O'Toole, G.A. (2011) Microtiter dish biofilm formation assay. *J Vis Exp* **47**: e2437.

522 Pardee, A.B., Jacob, F., and Monod, J. (1959) The genetic control and cytoplasmic  
523 expression of “inducibility” in the synthesis of b-galactosidase in *E. coli*. *J Mol Biol* **1**: 165–178.

524 Paul, R., Abel, S., Wassmann, P., Beck, A., Heerklotz, H., and Jenal, U. (2007) Activation of  
525 the diguanylate cyclase PleD by phosphorylation-mediated dimerization. *J Biol Chem* **282**:

526 29170–7.

527 Paul, R., Weiser, S., Amiot, N.C., Chan, C., Schirmer, T., Giese, B., and Jenal, U. (2004) Cell  
528 cycle-dependent dynamic localization of a bacterial response regulator with a novel di-  
529 guanylate cyclase output domain. *Genes Dev* **18**: 715–27.

530 Persat, A., Inclan, Y.F., Engel, J.N., Stone, H.A., and Gitai, Z. (2015) Type IV pili  
531 mechanochemically regulate virulence factors in *Pseudomonas aeruginosa*. *Proc Natl Acad  
532 Sci U S A* **112**: 7563–8.

533 Reichhardt, C., Jacobson, A.N., Maher, M.C., Uang, J., McCrate, O.A., Eckart, M., and  
534 Cegelski, L. (2015) Congo red interactions with curli-producing *E. coli* and native curli amyloid  
535 fibers. *PLoS One* **10**: e0140388.

536 Romling, U., Galperin, M.Y., and Gomelsky, M. (2013) Cyclic di-GMP: the first 25 years of a  
537 universal bacterial second messenger. *Microbiol Mol Biol Rev* **77**: 1–52.

538 Rossmann, F., Brenzinger, S., Knauer, C., Dörrich, A.K., Bubendorfer, S., Ruppert, U., *et al.*  
539 (2015) The role of FlhF and HubP as polar landmark proteins in *Shewanella putrefaciens* CN-  
540 32. *Mol Microbiol* **98**: 727–742.

541 Roy, A.B., Petrova, O.E., and Sauer, K. (2012) The phosphodiesterase DipA (PA5017) is  
542 essential for *Pseudomonas aeruginosa* biofilm dispersion. *J Bacteriol* **194**: 2904–15.

543 Ryan, R.P., Fouhy, Y., Lucey, J.F., Crossman, L.C., Spiro, S., He, Y.-W., *et al.* (2006) Cell-  
544 cell signaling in *Xanthomonas campestris* involves an HD-GYP domain protein that functions  
545 in cyclic di-GMP turnover. *PNAS* **103**: 6712–6717.

546 Rybtke, M.T., Borlee, B.R., Murakami, K., Irie, Y., Hentzer, M., Nielsen, T.E., *et al.* (2012)  
547 Fluorescence-based reporter for gauging cyclic di-GMP levels in *Pseudomonas aeruginosa*.  
548 *Appl Environ Microbiol* **78**: 5060–5069.

549 Schmidt, A.J., Ryjenkov, D.A., and Gomelsky, M. (2005) The ubiquitous protein domain EAL  
550 is a cyclic diguanylate-specific phosphodiesterase: enzymatically active and inactive EAL  
551 domains. *J Bacteriol* **187**: 4774–4781.

552 Schneider, C.A., Rasband, W.S., and Eliceiri, K.W. (2012) NIH Image to ImageJ: 25 years of  
553 image analysis. *Nat Methods* **9**: 671–5.

554 Semmler, A.B.T., Whitchurch, C.B., Leech, A.J., and Mattick, J.S. (2000) Identification of a  
555 novel gene, *fimV*, involved in twitching motility in *Pseudomonas aeruginosa*. *Microbiology*  
556 **146**: 1321–1332.

557 Simm, R., Morr, M., Kader, A., Nimtz, M., and Romling, U. (2004) GGDEF and EAL domains  
558 inversely regulate cyclic di-GMP levels and transition from sessility to motility. *Mol Microbiol*  
559 **53**: 1123–1134.

560 Turnbull, L., and Whitchurch, C.B. (2014) Motility assay: twitching motility. *Methods Mol Biol*  
561 **1149**: 73–86.

562 Wehbi, H., Portillo, E., Harvey, H., Shimkoff, A.E., Scheurwater, E.M., Howell, P.L., and  
563 Burrows, L.L. (2011) The peptidoglycan-binding protein FimV promotes assembly of the  
564 *Pseudomonas aeruginosa* type IV pilus secretin. *J Bacteriol* **193**: 540–550.

565 Yamaichi, Y., Bruckner, R., Ringgaard, S., Möll, A., Cameron, D.E., Briegel, A., et al. (2012) A  
566 multidomain hub anchors the chromosome segregation and chemotactic machinery to the  
567 bacterial pole. *Genes Dev* **26**: 2348–60.

568 Zhu, B., Liu, C., Liu, S., Cong, H., Chen, Y., Gu, L., and Ma, L.Z. (2016) Membrane  
569 association of SadC enhances its diguanylate cyclase activity to control exopolysaccharides  
570 synthesis and biofilm formation in *Pseudomonas aeruginosa*. *Environ Microbiol* **18**: 3440–  
571 3452.

572 **Figure Legends**

573 **Figure 1. DgcP interacts with FimV.** Schematic diagrams of DgcP (**A**) and FimV (**B**),  
574 showing the GGDEF domain of DgcP; the transmembrane region (TM), TPR motifs and the  
575 LysM domain of FimV. The red box in FimV corresponds to the prey fragment and lines show  
576 the regions cloned to confirm the interaction. The *E. coli* host strain BTH101 was  
577 cotransformed with pKTA25\_DgcP (full length) and pUT18\_FimV constructs, as indicated in  
578 the figure; the interactions were observed in MacConkey plates as red colonies (**C**) or  
579 measured using the  $\beta$ -galactosidase activity as a reporter. Data are the means  $\pm$  SD from  
580 three replicates (**D**).

581 **Figure 2. DgcP localizes at the cell poles in a FimV-dependent manner.** msfGFP was  
582 fusioned to DgcP full-length (1-670), its N-terminal (1-199) or the C-terminal (209-670)  
583 regions, as depicted (**A**). The full length protein localizes at the cell poles in the  $\Delta dgcP$   
584 background (**B, top panels**), but deletion of *fimV* leads to a loss of localization (**B, bottom**  
585 **panels**). The intensity of the GFP fluorescence was measured in 300 cells of each strains and  
586 a heat map of DgcP\_msfGFP localization was obtained with MicrobeJ, as described in  
587 Material and Methods (**C**).

588 **Figure 3. Mutation in *dgcP* affects biofilm formation.** PA14 and the  $\Delta dgcP$  strains were  
589 inoculated at  $OD_{600} = 0.05$  in 48 well polystyrene plates with the media shown and kept at  
590 30°C for 16 h without agitation. The medium was discarded and adherent cells were washed  
591 and stained with 1% crystal violet, washed and measured at  $OD_{595}$ . (**A**). The same procedure  
592 was carried out for the strains overexpressing DgcP in LB with 0.2% arabinose (**B**). 3D  
593 pictures resulting from CLSM after 16 h (**C**) and 72 h (**D**) of biofilm formation in LB at 30°C in  
594 an 8-well Lab-tek chambered coverglass system. Data in **A** and **B** are the means  $\pm$  SD from  
595 five replicates.

596 **Figure 4.  $\Delta dgcP$  mutant presents defects related to surface behaviors.** Cells were  
597 stabbed into the bottom of an agar plate by using a toothpick and incubated upright at 37°C  
598 overnight, followed by 48 h of incubation at room temperature. The medium was discarded  
599 and adherent cells stained with crystal violet (**A**). Diameter of the twitching colonies was  
600 measured in triplicates. Data are the means  $\pm$  SD (**B**). Light microscopy images of PA14 and  
601  $\Delta dgcP$  twitching colonies. Interstitial biofilms formed at the interface between a microscope  
602 slide coated in solidified nutrient media (Gelzan Pad) after four hours of colony expansion.  
603 The  $\Delta fimV$  mutant was used as a negative control of twitching (**C**). A silicon slide was placed  
604 upright in a culture tube and after the different time points cells at the air-liquid interface were  
605 washed, fixed and the spread of cells during the initial stages of biofilm formation was  
606 observed by FESEM (**D**).

607 **Figure 5. DgcP activity is FimV dependent.** Full-length wild type DgcP (pDgcP) or DgcP  
608 mutated in its GGDEF domain (pDgcP-GGAAF), only DgcP C-terminal wild-type region  
609 (pDgcP-Cterm) and WspR (pWspR) were overexpressed from the pJN105 vector in PA14,  
610  $\Delta dgcP$  and  $\Delta fimV$  backgrounds. Biofilm (**A**), swimming motility (**B**), c-di-GMP quantitation (**C**)  
611 and *cdrA* mRNA relative levels (**D**) were assayed. FimV, DgcP or both were expressed in *E.*  
612 *coli* and the EPS production was assessed in Congo red plates (**E**). Data are the means  $\pm$  SD  
613 from three replicates. \*,  $p<0.05$ ; \*\*,  $p<0.01$ ; \*\*\*,  $p<0.001$

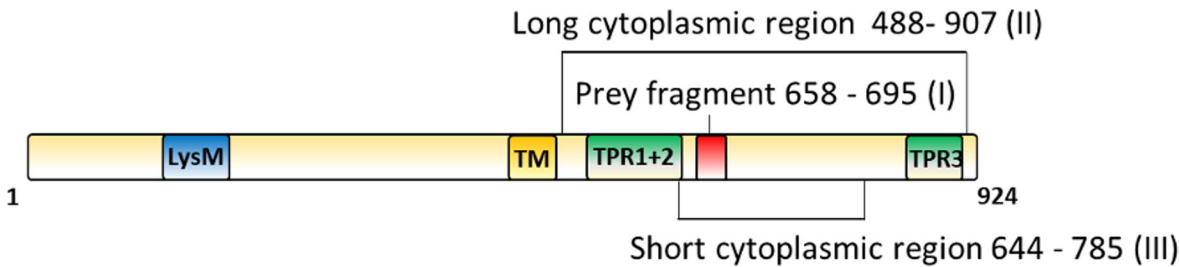
614 **Figure 6. Model of FimV-dependent localization and activity of DgcP.** In the PA14 wild  
615 type strain, DgcP is located at the pole due to interaction with FimV and may contribute to a  
616 local c-di-GMP pool (left). In a  $\Delta fimV$  background, DgcP is scattered in the cytoplasm and  
617 may have a small contribution to the global c-di-GMP pool (right). FimV, blue boxes; DgcP,  
618 green ellipses; c-di-GMP, red dots; nucleoid, blue dashed line; T4P, orange wavy lines and  
619 flagella, dark green lines.

620 **Figure S1. Multiple Sequence Alignment (MSA) and secondary structure prediction of**  
621 **DgcP homologues.** The MSA was generated using Muscle and edited in Jalview. The amino  
622 acids residues are colored using the Clustal X colour scheme. Secondary structure prediction  
623 was generated using JPred and is displayed as alpha-helices (red cylinders) and beta-sheets  
624 (green arrows) on the top of the alignment. Horizontal black bars represent the two putative  
625 N-terminal domains and the blue bar shows the GGDEF C-terminal domain. The orange  
626 vertical bar on the left point to *Pseudomonas* spp. and the purple bar groups other bacteria,  
627 as listed in **Table S1**.

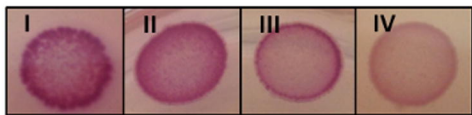
A



B

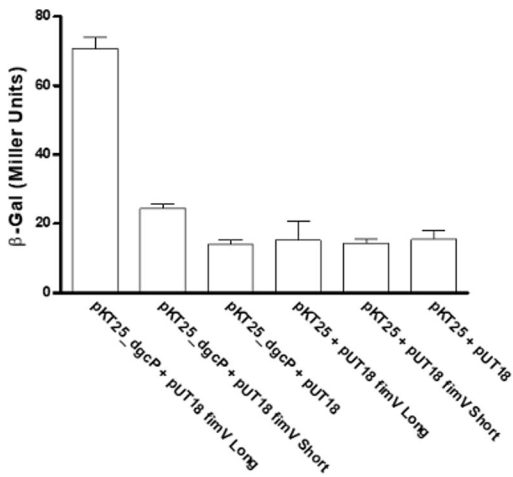


C

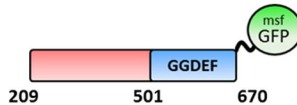
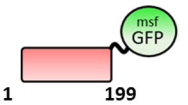


$pKT25$  -  $Dgcp$  +  $Prey$   
 $pKT25$  -  $dgcp$  +  $PUT18$   $fimV$   $Long$   
 $pKT25$  -  $dgcp$  +  $PUT18$   $fimV$   $Short$   
 $pKT25$  +  $PUT18$   $fimV$   $Long$

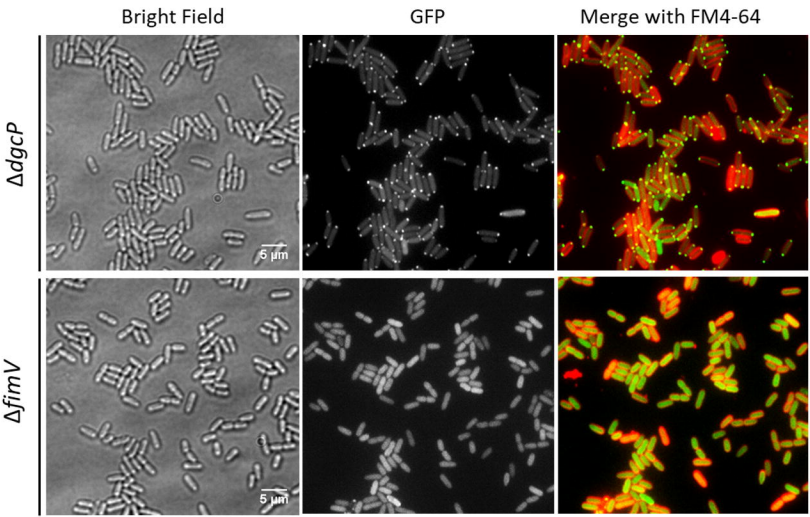
D



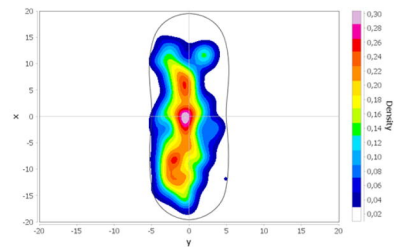
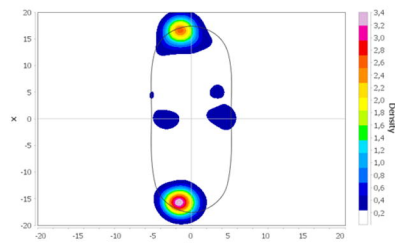
A

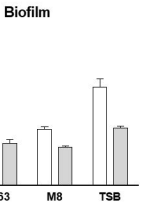
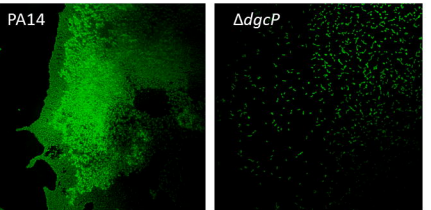
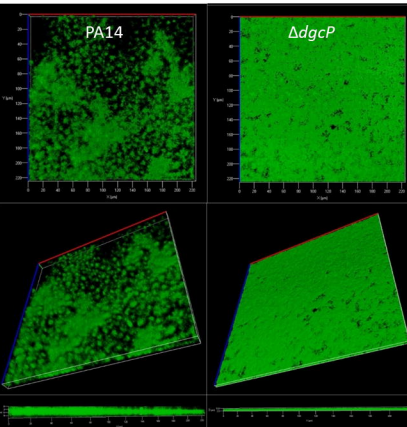
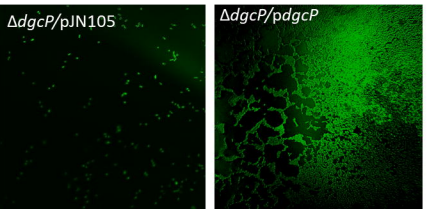
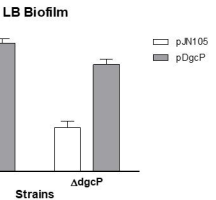


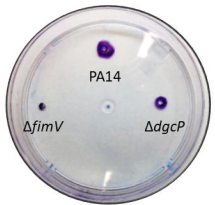
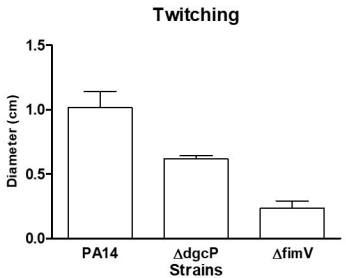
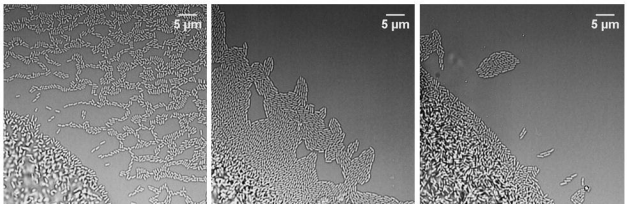
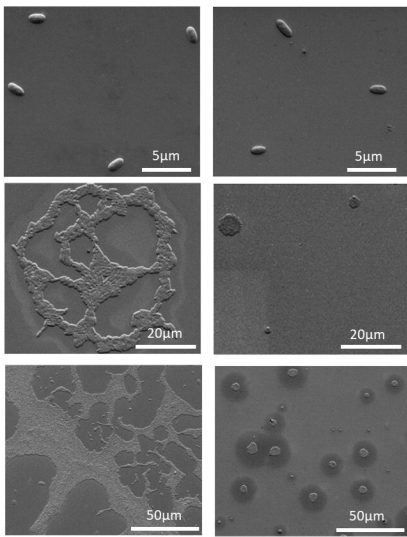
B



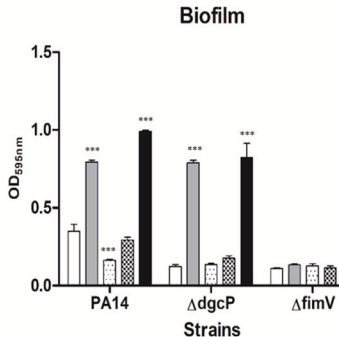
C



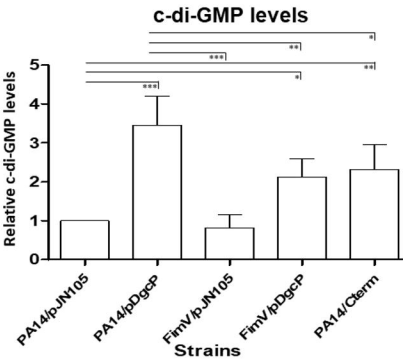
**A****C****16 Hours Biofilm****D****72 Hours Biofilm****B**

**A****B****C****D** $\Delta fimV$  $\Delta dgcP$  $\Delta fimV$

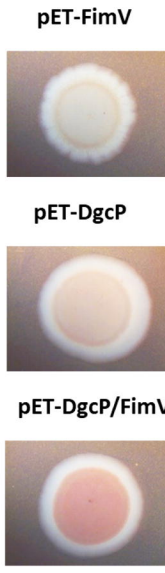
A



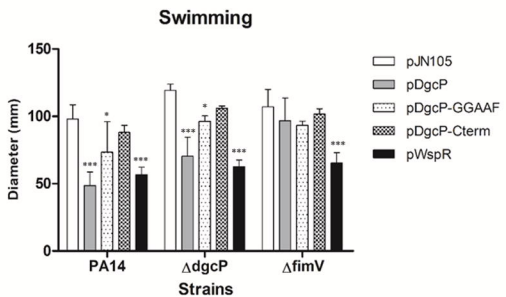
C



E



B



D

